22nd International Conference on Renewable Energies and Power Quality
(ICREPQ'24) Bilbao (Spain), 26th to 28th June 2024
Renewable Energy and Power Quality Journal (RE&PQJ)
ISSN 2172-038 X, Volume No.22, September 2024

Design of a recirculating water channel for the development of a hydrokinetic turbine

Betancour J.[1], Rubio-Clemente A.[1,2], Chica E.[1]

[1]Grupo de Investigación Energía Alternativa, Facultad de Ingeniería, Universidad de Antioquia UdeA, Calle 70, No. 52-21, Medellín, Colombia.
[2]Escuela Ambiental, Facultad de Ingeniería, Universidad de Antioquia UdeA, Calle 70, No. 52-21, Medellín, Colombia.

Phone/Fax number: +57 2195547

Abstract
This study presents the design, construction, and operational details of an experimental recirculating water channel dedicated to the assessment of hydrokinetic turbines, including a propeller-type turbine and a H-Darrieus turbine, since it offers a controlled testing environment. The recirculating water channel had overall dimensions of 5 m in length, 0.35 m in width, and 0.5 m in depth, it allows for the replication of various water flow conditions and permits a maximum achievable flow velocity of 0.6 m/s, which closely resembles real-world scenarios. Afterwards, a propeller-type turbine and a H-Darrieus turbine underwent characterization within the channel, and a performance curve constructed through the coefficient versus the blade tip speed ratio (TSR) revealed a peak efficiency of 0.2129 at a TSR of 2.952 for the propeller turbine, and a higher peak efficiency of 0.3076 at a TSR of 0.38 for the H-Darrieus turbine. The versatility of this experimental setup makes it a valuable platform for in-depth performance studies of hydrokinetic turbines. This water channel and its systematic characterization process represent a vital resource for conducting efficiency and behavior analyses across a wide range of operational parameters related to hydrokinetic turbine technologies.

Key words. renewable energy, recirculating water channel, hydrokinetic turbine, experimental test methodology.

1. Introduction
Given the increasing global demand for energy, the imperative to shift towards renewable sources becomes more apparent. As societies expand and reliance on technology deepens, the strain on traditional fossil fuel-based power generation becomes unsustainable [1,2]. Thus, there is a critical need for the transition to renewable energy solutions like solar, wind, and hydroelectric power. These sources provide cleaner, and more sustainable ways to meet energy needs, reducing greenhouse gas emissions, and combating climate change [3, 4, 5].
Hydrokinetic turbines play a vital role in diversifying the energy matrix, offering unique advantages, and facing specific challenges. They harness the kinetic energy of water currents, providing a renewable and predictable energy source, reducing reliance on fossil fuels. Their minimal environmental impact and scalability make them suitable for various settings, from rivers to oceans. However, challenges include variable energy production due to fluctuating water currents and potential impacts on aquatic ecosystems. Nonetheless, hydrokinetic turbines are promising for sustainable, diversified energy sources [6,7,8].

The development of hydrokinetic turbines is a dynamic field of research, with the potential to significantly contribute to diversifying the energy matrix. To optimize turbine rotor design, researchers combine numerical simulations and experimental studies. Numerical simulations offer insights into turbine performance by modelling and predicting its behaviour under various conditions. Despite their accuracy, experimental studies are crucial for validating these results. Physical testing in controlled environments, such as water channels or test facilities, confirms numerical predictions and provides essential real-world performance data [10].
Well-equipped experimental facilities are crucial for this process, serving as testbeds for experiments under various flow conditions. They bridge the gap between theoretical predictions and practical performance, allowing researchers to refine the turbine design and optimize its efficiency.
In the literature, numerous experimental investigations have leveraged water channels for the assessment of hydrokinetic turbines. Nevertheless, a notable gap often exists regarding the comprehensive detailing of the design and construction aspects of these experimental facilities. As such, this study aims to fulfil the need for an in-depth exposition by presenting a thorough account of the design process, equipment selection, and the construction methodology employed in the establishment of a specialized water channel tailored for the experimentation and performance evaluation of hydraulic turbines. Additionally, this work expounds upon the intricacies of the measurement systems integrated into the experimental setup, elucidating their roles and functionalities. The study delves into the process of turbine characterization, systematically delineating the procedures and methodologies adopted, with the overarching goal of plotting the turbine performance curve. This curve, commonly represented as the power coefficient versus the tip speed ratio, is crucial in elucidating the turbine

efficiency and behaviour across a range of operational conditions.

2. Materials and methods

The technical design of a recirculating water channel for hydrokinetic turbine testing necessitates meticulous attention to various aspects. The channel dimensions must be sufficiently expansive to accommodate the turbines and facilitate the realistic recreation of flow conditions. The cross-sectional shape of the channel, whether an open test section rectangular or trapezoidal, should promote efficient water circulation. A uniform velocity distribution should be achieved in the test section. The incorporation of a flow control system is imperative for the variation and maintenance of flow velocities in accordance with the study requirements. Precision measurement is essential, and high-quality measurement systems must be installed to record data such as water velocity, pressure, and generated power accurately. Turbine mounting systems need to be adaptable, allowing variations in the attack angles to evaluate various turbine designs. Moreover, real-time monitoring and control systems are pivotal for *in situ*, real-time assessment of test conditions. The phase of initial dry testing and adjustments is paramount to ascertain the proper functioning of all systems. The turbine testing phase involves turbine installation and the evaluation of their performance under various flow conditions. Post-test data analysis is fundamental for comprehending the turbine behaviour and making improvements to the design and testing conditions.

Designing a water recirculation system for hydrokinetic turbine testing involves considering various aspects, from the location of reservoirs to the selection of the pumping system and the geometry of the test channel. Below, a basic sequence for the design is described:

Step 1: Definition of requirements and constraints.

• Establishing the operational parameters, such as the range of water velocity. In the design of the channel in Alternative Energy research group at University of Antioquia, a maximum current velocity of 0.6 m/s was set for the test section of the column.

• Defining the area that can be used for the location of the experimental setup. The available area in the channel referred above was 10.5 m^2 and was characterized by a width and length of 1.5 m and 7 m, respectively. The area where the experimental setup would be installed must have access to a water source and a drainage system for maintenance purposes.

• Implementing safety measures where possible, such as railings and signage, to ensure a safe working environment.

• Assuring that the experimental setup allows for the recirculation of water used in tests to minimize waste.

Step 2: Pumping system design

• Creating a diagram of the overall configuration of the test setup, identifying the components to be designed and/or selected. Fig. 1 shows the general configuration design of the experimental installation.

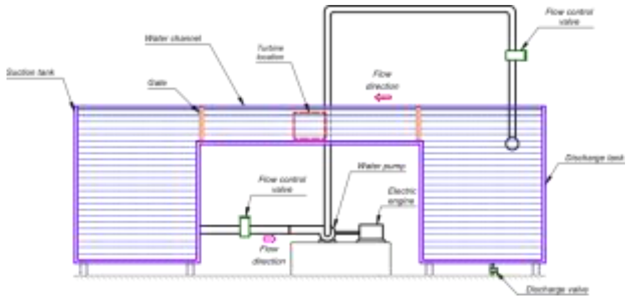

Fig 1. General configuration design of the experimental installation

• Selecting the pump and network of pipes and valves to deliver the required flow rate for hydrokinetic turbine experimental tests.

Starting with the requirements for the desired maximum velocity and the floodable area of the channel (defined in step 3), the necessary flow rate in the system is determined; this flow rate is 0.073 m^3/s and is equivalent to 1165 GPM. With this information, the goal is to find a pump that delivers 1200 GPM, slightly more than the calculated amount.

With the selected 1200 GPM and considering recommendations for water velocities in pumping systems, pipe diameters are chosen to be used. A 10" diameter is selected for the pump suction, and an 8" diameter, for the discharge. This results in velocities of 1.4 and 2.28 m/s, respectively, figures that fall within the ranges recommended by the National Standard Plumbing Code for water distribution piping within buildings. The code suggests sizing pipelines for a maximum velocity of 8 feet per second (2.438 m/s) at the design flow rate unless the pipe manufacturer recommends a lower maximum velocity. Exceeding this limit could increase the risk of water hammer and pipe movement due to abrupt changes in water momentum. Water hammer, also known as hydraulic shock, occurs in plumbing systems when there is a sudden change in water flow velocity. This phenomenon arises when swiftly moving water is abruptly halted or forced to change direction, causing a rapid surge in pressure within the pipe.

Once the pipe dimensions are determined, it is possible to outline the design of the system, which is depicted in Fig. 2.

The recirculating water channel made up of suction (1) and discharge (11) tank, suction pipe (2), two gate valves (3, and 9), one eccentric reducer of 10x6 in for suction (4), a pump (5), a motor (6), a concentric reducer of 8x5 in for discharge (7), a check valve (8), and a discharge pipe (10).

For the pumping system, the centrifugal pump selected is the GRUNDFOS model NK 125-200/176-154 EUP A1F2AE-SBAQE, featuring a hydraulic point of 1200 GPM @ 9.8 m and a required net positive suction head ($NPSH_{req}$) of 5.83 m. The pump connections on the suction and discharge sides are made with DN 150x125 DIN flanges. The pump mechanical seal consists of carbon/silicon/EPDM, and both the casing and impeller are made of cast iron. The motor power and operating speed are 15 HP and 1800 rpm, respectively.

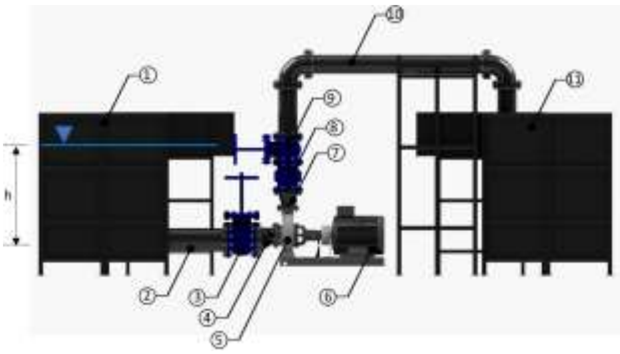

Fig. 2. Detail of the pumping system components. 1) Suction tank, 2) suction pipe, 3) gate valve, 4) eccentric reducer, 5) pump, 6) motor, 7) concentric reducer, 8) check valve, 9) gate valve, 10) discharge pipe, 11) Discharge tank

It is important to calculate the net positive suction head available ($NPSH_a$) of the pump to prevent cavitation and protect the pumping system components. The $NPSH_a$ is a crucial factor influencing the pump efficiency and the overall performance. Its computation involves establishing the suction head loss (Hs) and the available head at suction (H_a). The $NPSH_a$ is then determined by subtracting Hs from H_a, as per the formula expressed in Eq. (1).

$$NPSH_a = H_a - H_s \quad (1)$$

The $NPSH_a$ must exceed the minimum NPSH specifications of the pump design to avoid cavitation. It is crucial to execute these computations meticulously, taking into account the pump unique operating conditions, including the fluid velocity and the suction pipe geometry. The calculation of H_s can be conducted using Eq. (2).

$$H_s = \frac{V^2}{2g} + h_f + h_v \quad (2)$$

In this context, V represents the fluid velocity within the suction pipe, g denotes the acceleration due to gravity, h_f accounts for head loss attributed to friction, and hv reflects the head loss resulting from restrictions at the pump inlet. Conversely, the determination of Ha can be accomplished through the utilization of Eq. (3).

$$H_a = P_{atm} + h \quad (3)$$

where P_{atm} is the atmospheric pressure, h is the manometric height above the free surface of the fluid. For this design, there is an available $NPSH_a$ of 6.19 m and losses in the discharge of 3 m. Hence, under the given operating conditions of the channel, the pump will not experience cavitation.

• Designing a control system for the pumping system that allows for the regulation of the flow rate and, consequently, the velocity in the test channel. The control system design for a compound pump, incorporating a Programmable Logic Controller (PLC) and a variable frequency drive (VFD), serves to regulate the operational range of the pump, facilitating multiple water circulation speeds. The integration of a PLC allows for the precise and programmable control of the pump operation, enabling efficient adjustments to meet varying operational requirements. Coupled with a VFD, the pump can achieve different speeds, providing flexibility in water circulation applications. The control interface shown in Fig. 3 and developed using LabVIEW, enhances user accessibility by allowing seamless adjustments to the pump operational range. This intuitive interface enables operators to set and modify parameters with ease, ensuring optimal performance. Additionally, the system incorporates emergency stop protection mechanisms to promptly halt pump operations in critical situations, enhancing safety measures.

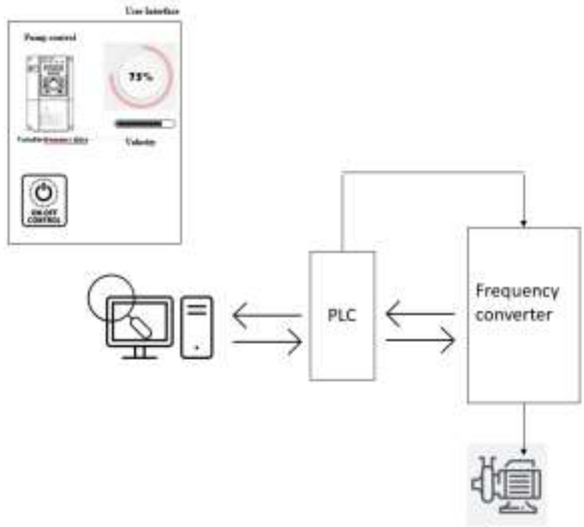

Fig. 3. Control system interface for the pumping system

• Defining the capacity of the reservoirs to ensure a constant water flow in the water channel. The suction and discharge tanks have a L form, made of steel both with a 1.5 m^3 water capacity.

Step 3: Test channel design

• Determining the dimensions of the test channel or the connecting channel between the two reservoirs. It is recommended to use a rectangular or trapezoidal channel to simulate realistic flow conditions. The dimensions of the channel influence the size of the turbines to be evaluated. Therefore, laboratory-scale turbine models should be sized according to the cross-sectional area of the channel to avoid the influence of channel walls in experimental tests. A channel section with a width, height, and length of 0.35, 0.5 and 5 m, respectively, has been defined. These cross-sectional dimensions align with values used by other researchers [11, 12, 13]. The water recirculation channel, extending from the discharge tank to the suction tank, features a transparent acrylic window on one of its walls. This allows for the visualization of the turbine behavior within the flow.

Step 4: Control and monitoring system

• Adopting appropriate instrumentation for the measurement of speed, torque, and angular velocity to characterize the turbines. To quantify the turbine power, torque sensors equipped with encoders will be utilized, along with a braking system for applying load to the turbine. This system enables the creation of an efficiency curve, showcasing the turbine performance under varying conditions. The incorporation of torque sensors with encoders ensures precise measurement of the turbine developed torque, while the braking system simulates different operational scenarios, assessing efficiency across various loads. This comprehensive approach facilitates an accurate power measurement, providing valuable insights into the turbine efficiency characteristics.

• Establishing a real-time monitoring system for observing test data and making necessary adjustments. The implementation of a real-time monitoring system is crucial for effectively observing and adjusting test data during experiments. This can be achieved through a data acquisition system continuously recording sensor data. By utilizing software platforms such as MATLAB, the system processes and displays the turbine characteristic curves in real-time. This allows researchers and engineers to promptly analyze performance metrics, identify trends, and make necessary adjustments to optimize turbine operation. With this setup, the testing process becomes dynamic and responsive, enhancing the overall efficiency of data collection and analysis throughout the experiments.
The comprehensive costs of the experimental installation are presented in Table 1. The total cost of the installation amounted to 19,260 USD.

Table 1. Total cost of the recirculating water channel

Components	Cost (USD)
Pumps, 1 non-rising stem gate valve for suction and another for discharge, both of 10 and 8 inches. 1 check valve of 8 inches. 1 eccentric reducer of 10x6 inches for suction and a concentric reducer of 8x5 inches for discharge.	7,140
Suction and discharge pipe	3,570
Suction and discharge tanks, support structure, and recirculation channel	8,550
Total	19,260

Fig. 4 illustrates the overall dimensions of the designed water recirculation channel that were achieved through the systematic implementation of the four outlined steps. The structure of the water recirculation channel was fabricated using square structural tubing of 1.5 inches, A36 steel sheet with a gauge of 14, and angles of 1.5 inches by 1/8 inches. The structure was painted with a corrosion-resistant epoxy paint.

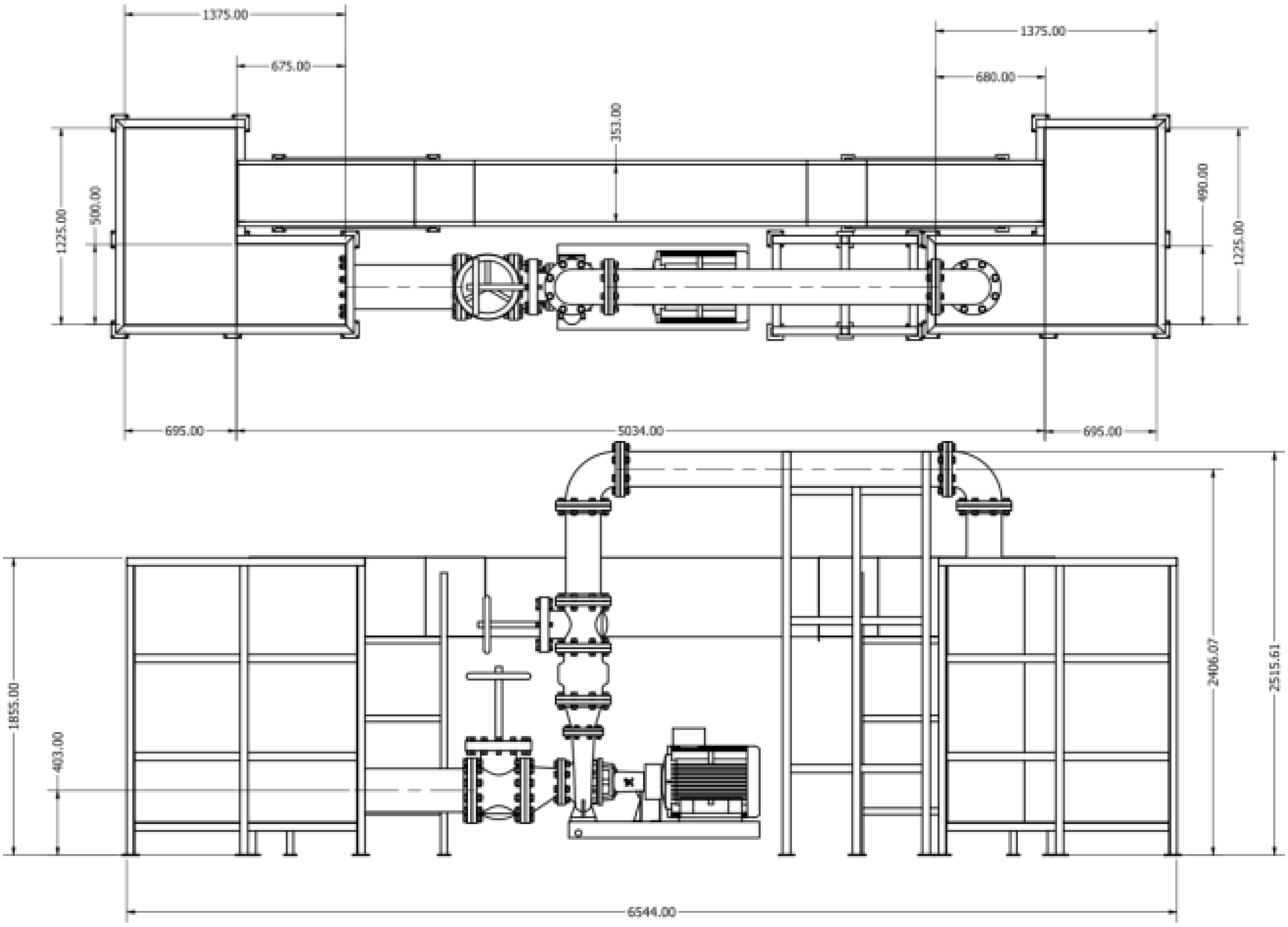

Fig. 4. Overall dimensions of the experimental installation. Measurements are expressed in mm

The experimental characterization of the two hydrokinetic turbines was conducted within the specially designed water recirculation channel. The turbines under investigation included a horizontal-axis hydrokinetic turbine (HAHT) and a vertical-axis hydrokinetic turbine (VAHT), depicted in Fig. 5a and 5b, respectively. The HAHT, functioning as a propeller turbine, featured a rotor with a diameter (D) of 0.24 m, along with a skew angle of 13.3° and a rake angle of -18.06°. On the other hand, the VAHT was a H-Darrieus turbine with dimensions including a D of 187.5 mm, height (H) of 141 mm, and chord length (C) of 42.5 mm. The H-Darrieus turbine incorporated a NACA 0015 hydrofoil with an angle of attack set at -10°. Both turbines, each equipped with three blades, were fabricated using a 3D-printer system.

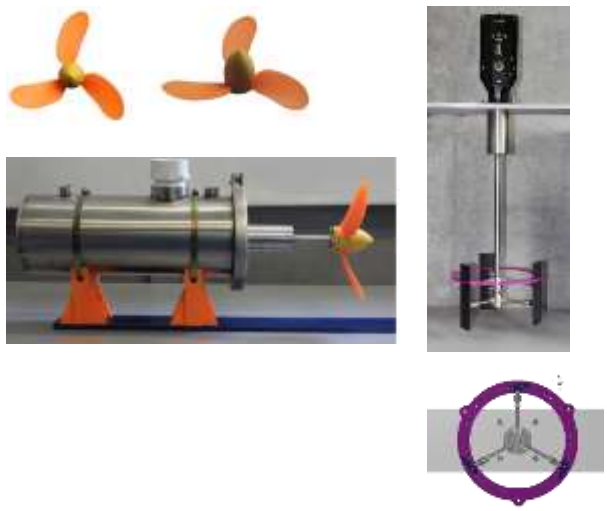

a) b)

Fig. 5. a) Propeller hydrokinetic turbine, b) H-Darrieus hydrokinetic turbine

The evaluation of the turbine performance involved the utilization of the coefficient of performance (C_P), a metric indicating the turbine efficiency. C_P was determined by the ratio of the turbine power output to the maximum power available in the free-stream tube of a cross-sectional area (A), and its calculation was articulated in Eq. (4). In the case of the HAHT, A corresponds to the rotor swept area, represented by πR^2. For the VAHT, A is computed by multiplying the rotor H and D [9, 10, 14].

$$C_p = \frac{T\omega}{\frac{1}{2}\rho A V^3} \tag{4}$$

where, T represents the torque, ρ denotes the water density, ω is angular velocity, and V is the water free stream velocity. Simultaneously, the tip speed ratio (TSR) is characterized as the proportion between the tangential speed of the blade tip and the upstream flow velocity [9, 14, 15]. The calculation of TSR is governed by Eq. (5), with R representing the turbine radius.

$$TSR = \frac{R\omega}{V} \tag{5}$$

The representation of the turbine performance is commonly depicted through a graph of C_P vs. TSR. The theoretical maximum C_P value stands at 0.593 for a single and open actuator disc, a constraint acknowledged as the Betz limit. This limit is grounded in the understanding that a turbine relies on the fluid movement for power generation, and excessive extraction of the kinetic energy would impede its operation [9, 14].

The experimental setup took place in a recirculation channel. A flowmeter (FlowWatch FW450) with an accuracy of ±0.01 m/s was employed for the water speed measurement. Measurements were conducted at three positions upstream of the rotor, and the averaged values were used. T and ω were measured using a torque sensor (Futek-Model TR605) with an encoder (accuracy of 0.000110 Nm and >10,000 Cpr, respectively). Real-time data recording was facilitated by the intelligent digital display (IHH500 pro) connected to the sensor. For HAHT measurements, the torque sensor and data acquisition system were submerged in a water-resistant vessel, as depicted in Fig. 5a. In the case of VAHT, the sensor was positioned above the water surface.

To assess the torque generated by the turbine across various TSRs, a braking system connected to one end of the torque sensor was employed. This system utilizes a direct current motor and a reverse current braking approach, wherein the electric motor functions as a brake in the turbine model. It sustains the turbine model operation at a consistent TSR. The approach involves energizing the DC motor in the opposite direction to the turbine rotation, creating a reactive torque that counters the turbine ω and reduces it. Simultaneously, the motor operates as an electric generator, slowed down by the power demand of the system. The braking torque is fine-tuned based on the desired turbine ω, regulating the current flow to the DC motor through pulse width modulation (PWM). In this system, a microcontroller and a power coupling circuit achieved this regulation, coupling the microcontroller signal with the DC motor power supply. When a decrease (or increase) in the turbine ω is needed, the microcontroller adjusted the PWM duty cycle, subsequently altering the energy supplied to the motor and, consequently, the braking torque [16].

The turbine models underwent testing in a uniform steady flow to establish their characteristics through a non-dimensional power performance curve correlating C_P with TSR. To achieve this, the rotors were aligned perpendicularly to the flow direction. C_P values were computed using Eq. (4), with the water fixed free stream velocity (~ 0.5 m/s), and ω was controlled to attain various TSR values. All results were obtained for the two rotor configurations under study.

3. Results and discussion

Fig. 6 compares the turbine performances obtained from the experiments. The results indicated a C_P peak of 0.3076 at a λ of 0.380 for the H-Darrieus turbine. In contrast, a C_P of 0.2129 at a λ equal to 2.952 was recorded for the propeller turbine. To harness electrical energy, generators coupled to the turbine typically operate at specific RPM levels, usually at high RPM. Given that hydrokinetic turbines, especially the current H-Darrieus turbine, generate power at low RPM, incorporating a gearbox between the turbine and the generator becomes necessary. This gearbox serves to elevate the ω from the turbine low-speed main shaft to a high-speed shaft, effectively linking with an electrical generator.

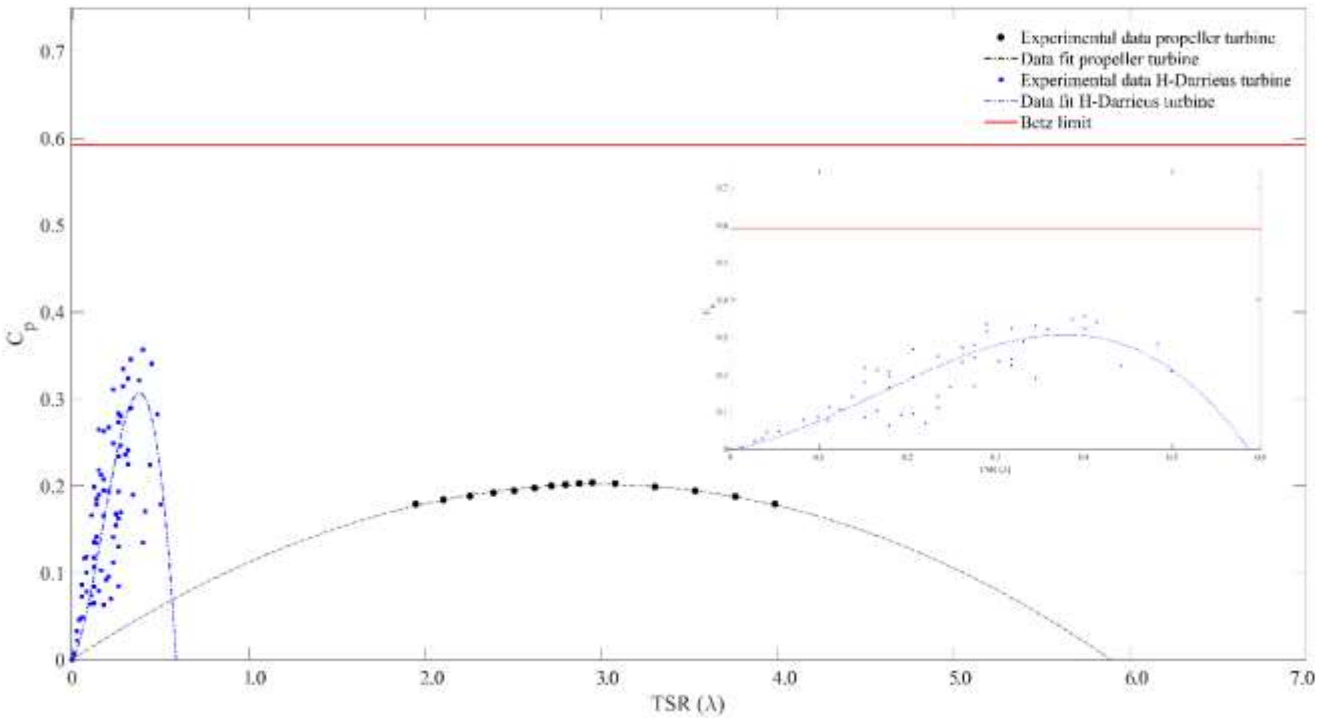

Fig. 6. Power coefficient (C_p) *vs.* tip speed ratio (TSR) values

The C_P of the H-Darrieus turbine was notably higher compared to that of the propeller hydrokinetic turbine. The H-Darrieus design exhibited a simpler structure than the propeller turbine, as the latter blade featured a more intricate geometry, demanding precision in machining and manufacturing. Consequently, the straightforward design of the H-Darrieus turbine positively impacts the manufacturing process, potentially leading to a reduction in total costs. In the case of a propeller turbine, both the gear and the generator need to be submerged underwater. Conversely, in a VAHT, the generator can be attached to one end of the shaft, allowing it to be positioned above water and potentially lowering costs associated with water-sealed technology [9, 10 15]. Despite the advantages of the H-Darrieus turbine, it exhibits suboptimal starting characteristics and a less stable ω when compared to the propeller turbine. Additionally, the H-Darrieus turbine blades undergo an unstable peak load during operation, potentially causing vibrations and reducing its overall lifespan. As a result, the use of a propeller turbine is recommended for power generation in developing countries.

4. Conclusion

The design and implementation of a water recirculation channel for the testing of hydrokinetic turbines in a controlled environment signify a pivotal step towards advancing sustainable and efficient technologies. The establishment of such an experimental facility is crucial for systematically evaluating the performance and efficiency of hydrokinetic turbines. This controlled setting allows for accurate measurements and assessments, providing valuable insights for the development of innovative and sustainable solutions in the field of renewable energy. Furthermore, the adaptability of the water channel allows for the evaluation of different turbine models, promoting a thorough exploration of their capabilities and enriching the broader understanding of hydrokinetic energy conversion technologies. This facility stands as a foundational element for research and development, providing a launchpad for the advancement of environmentally sustainable and impactful energy solutions.

Moreover, the results suggest that both turbines have the potential to make substantial contributions to Colombia's future renewable energy landscape. The H-Darrieus turbine exhibits a C_P approximately 44.44% higher than that of the propeller turbine, with the latter presenting a comparatively lower C_P. However, the propeller turbine features a higher ω and less fluctuation in T, mitigating structural concerns within the turbine.

Acknowledgement

The authors gratefully acknowledge the financial support provided by the Colombian Ministry of Science, Technology, and Innovation “MinCiencias” through "Patrimonio Autónomo Fondo Nacional de Financiamiento para la Ciencia, la Tecnología y la Innovación, Francisco José de Caldas" (Perseo Alliance, Contract No. 112721-392-2023).

References

[1] Bei, J., & Wang, C. (2023). Renewable energy resources and sustainable development goals: Evidence based on green finance, clean energy and environmentally friendly investment. Resources Policy, 80, 103194.

[2] Xue, C., Shahbaz, M., Ahmed, Z., Ahmad, M., & Sinha, A. (2022). Clean energy consumption, economic growth, and environmental sustainability: what is the role of economic policy uncertainty?. Renewable Energy, 184, 899-907.

[3] Olabi, A. G., & Abdelkareem, M. A. (2022). Renewable energy and climate change. Renewable and Sustainable Energy Reviews, 158, 112111.

[4] Jaiswal, K. K., Chowdhury, C. R., Yadav, D., Verma, R., Dutta, S., Jaiswal, K. S., & SelvaKumar, K. K. (2022). Renewable

and sustainable clean energy development and impact on social, economic, and environmental health. Energy Nexus, 100118.
[5] Perez, A., & Garcia-Rendon, J. J. (2021). Integration of non-conventional renewable energy and spot price of electricity: A counterfactual analysis for Colombia. Renewable Energy, 167, 146-161.
[6] Espina-Valdés, R., Fernández-Álvarez, V. M., Gharib-Yosry, A., Fernández-Jiménez, A., & Álvarez-Álvarez, E. (2022). Increased efficiency of hydrokinetic turbines through the use of an obstacle on the channel bottom. Ocean Engineering, 266, 112872.
[7] Guner, F., & Zenk, H. (2020). Experimental, numerical and application analysis of hydrokinetic turbine performance with fixed rotating blades. Energies, 13(3), 766.
[8] Khan, R., & Kumar, A. (2023). Performance enhancement of hydrokinetic turbine using augmentation techniques: a review. International Journal of Green Energy, 1-28.
[9] Niebuhr, C. M., Schmidt, S., van Dijk, M., Smith, L., & Neary, V. S. (2022). A review of commercial numerical modelling approaches for axial hydrokinetic turbine wake analysis in channel flow. Renewable and Sustainable Energy Reviews, 158, 112151.
[10] Niebuhr, C. M., Van Dijk, M., Neary, V. S., & Bhagwan, J. N. (2019). A review of hydrokinetic turbines and enhancement techniques for canal installations: Technology, applicability and potential. Renewable and Sustainable Energy Reviews, 113, 109240.
[11] Álvarez-Álvarez, E., Rico-Secades, M., Fernández-Jiménez, A., Espina-Valdes, R., Corominas, E. L., & Calleja-Rodríguez, A. J. (2020). Hydrodynamic water tunnel for characterization of hydrokinetic microturbines designs. Clean Technologies and Environmental Policy, 22, 1843-1854.
[12] Nedelcu, A., Bunea, F., Danca, P. A., Chihaia, R. A., Babutanu, C. A., Marin, D., & Ciocan, G. D. (2021, May). Experimental research on a hydrokinetic turbine model. In IOP Conference Series: Earth and Environmental Science (Vol. 664, No. 1, p. 012061). IOP Publishing.
[13] Ferraiuolo, R., Gharib-Yosry, A., Fernández-Jiménez, A., Espina-Valdés, R., Álvarez-Álvarez, E., Del Giudice, G., & Giugni, M. (2022). Design and Experimental Performance Characterization of a Three-Blade Horizontal-Axis Hydrokinetic Water Turbine in a Low-Velocity Channel. Environmental Sciences Proceedings, 21(1), 62.
[14] Nunes, M. M., Mendes, R. C., Oliveira, T. F., & Junior, A. C. B. (2019). An experimental study on the diffuser-enhanced propeller hydrokinetic turbines. Renewable Energy, 133, 840-848.
[15] Tan, K. W., Kirke, B., & Anyi, M. (2021). Small-scale hydrokinetic turbines for remote community electrification. Energy for Sustainable Development, 63, 41-50.
[16] Betancour, J., Romero-Menco, F., Velásquez, L., Rubio-Clemente, A., & Chica, E. (2023). Design and optimization of a runner for a gravitational vortex turbine using the response surface methodology and experimental tests. Renewable Energy, 210, 306-320.